Authors' accepted manuscript.
Article published in *Clinical Biomechanics*, Volume 92, February 2022, 105552
Final published version available at https://doi.org/10.1016/j.clinbiomech.2021.105552

Cervical spine injury response to direct rear head dynamic impact

Marie-Hélène Beauséjour [a,b,c,d], Yvan Petit [a,b,c], Éric Wagnac [a,b,c], Anthony Melot [c,d,e], Lucas Troude [f], Pierre-Jean Arnoux [c,d]

[a] Department of Mechanical Engineering, École de technologie supérieure, 1100 Notre-Dame Street West, H3C 1K3, Montreal, Quebec, Canada

[b] Research Center, Hôpital du Sacré-Coeur de Montréal, 5400 Boulevard Gouin, H4J 1C5, Montreal, Quebec, Canada

[c] International Laboratory on Spine Imaging and Biomechanics, France and Canada

[d] Laboratoire de Biomécanique Appliquée-Université Gustave-Eiffel, Aix-Marseille Université, UMR T24, 51 boulevard Pierre Dramard, 13015, Marseille France

[e] Hôpital privé Clairval, 317 boulevard du Redon, 13009, Marseille, France

[f] Neurosurgery, CHU Nord Marseille, Chemin des Bourrely, cedex 20,13015, Marseille, France

Corresponding author:
Yvan Petit
e-mail address: yvan.petit@etsmtl.ca
Address: 1100 Notre-Dame Street West, H3C 1K3, Montreal, Quebec, Canada

Abstract

Background: Direct rear head impact can occur during falls, road accidents, or sports accidents. They induce anterior shear, flexion and compression loads suspected to cause flexion-distraction injuries at the cervical spine. However, post-mortem human subject experiments mostly focus on sled impacts and not direct head impacts.

Methods: Six male cadavers were subjected to a direct rear head impact of 3.5 to 5.5 m/s with a 40 kg impactor. The subjects were equipped with accelerometers at the forehead, mouth and sternum. High-speed cameras and stereography were used to track head displacements. Head range of motion in flexion-extension was measured before and after impact for four cadavers. The injuries were assessed from CT scan images and dissection.

Findings: Maximum head rotation was between 43 degrees and 78 degrees, maximum cranial-caudal displacement between -12 mm and -196 mm, and antero-posterior displacement between 90 mm and 139 mm during the impact. Four subjects had flexion-distraction injuries. Anterior vertebral osteophyte identification showed that fractures occurred at adjacent levels of osteophytic bridges. The other two subjects had no anterior osteophytes. They suffered from C2 fracture and one subject had a C1-C2 subluxation. C6-C7 was the most frequently injured spinal level.

Interpretation: Anterior vertebral osteophytes appear to influence the type and position of injuries, while osteophytes would seem to provide stability in flexion for the osteoarthritic cervical spine, but to also lead to stress concentration in levels adjacent to the osteophytes. Clinical management of patients presenting with osteophytes fracture should include neck immobilization and careful follow-up to ensure bone healing.

Keywords: Cervical spine; flexion-distraction, trauma; osteophyte; head-first impact

1. Introduction

Rear head impact can occur in different situations, including motorcycle or bicycle accidents (Bourdet et al., 2014; Molinero, 2013), car and pedestrians collisions (Yin, Li and Xu, 2017) and sports accidents (Dennison, Macri and Cripton, 2012; Bailly et al., 2018). This type of head impact generates flexion and compression loads on the spine (King, 2018, p. 209; Viano and Parenteau, 2008). Nightingale et al. (2019) postulated that compression and compression buckling are the main mechanisms of cervical spine dislocation than hyperflexion. Dislocation is a serious correlated with a high risk of spinal cord injury (Mattucci et al., 2019). Dislocation and subluxation is the most severe stage of flexion-distraction type injuries, which are characterized by rupture of the posterior ligamentous complex and intervertebral disc (IVD) with or without bony fracture (Izzo et al., 2019). Flexion-distraction injuries are common at the cervical spine and are associated with neurological deficits in 61%

of cases (Blauth et al., 2007). It is therefore important to characterize the mechanisms leading to flexion-distraction injuries to better understand them and design more efficient safety devices to counter them. However, studies on direct head impacts, which are susceptible to lead to flexion-distraction injuries, are few and are rarely performed on full body specimens.

Several studies on cervical spine trauma due to head loading have used specimens composed of the complete cervical spine, with the head or an artificial head. Some previous studies performed axial loading to the head with an hydraulic testing device (Maiman, Yoganandan and Pintar, 2002; Pintar et al., 1998; 1990). Maiman et al. (2002) and Pintar et al. (1998) observed cases of flexion-distraction injury due to axial compression loading of the head. However, this scenario is not necessarily representative of the transient loading experienced during real-life accidents. Regarding the injuries, Pintar et al. (1990) mostly produced vertebral body fractures since they straightened the cervical spine before loading. Ivancic (2012) simulated head impact by propelling cervical spine specimens incorporating a surrogate head to a wall with a forward head protrusion. All ten of their osteo-ligamentous specimens sustained injuries to the posterior ligamentous complex at C7-T1. However, muscles and soft tissues were removed from the specimens and the fixation at T1 may have increased the loads sustained at the C7-T1 functional spinal unit (FSU). Using five post-mortem human subjects (PMHS), Pintar et al. (2010) performed frontal sled impact. Three specimens had lower cervical spine dislocation at C6-C7 or C7-T1 accompanied with vertebral body fractures, but this test corresponds to a different mechanism than direct head impact. Three different studies examining neck compression injuries following impact to the top of head performed on PMHS were analyzed by Viano and Parenteau (2008). Merging the results of the three tests studies, it was shown that head velocity is linked to impact force and risk of serious injury. There is, however, a dearth of kinematics and injury data direct rear head impacts in the literature.

While the PMHS used in experimental studies are often old and susceptible to osteoarthrosis, the osteophytes influence on cervical spine injuries has never been investigated. Spinal segments with osteophytes are stiffer under axial loading and exhibit a higher load at failure (Wagnac et al., 2017). Osteophytes at the thoracolumbar spine restrain movements, especially bending (Al-Rawahi et al., 2011). It is therefore conceivable that osteophytes could protect

the spine from trauma by limiting movement. In a clinical study of cervical spine injury among professional wrestlers, Sasaki et al. (2018) observed that for patients with large anterior osteophytes, spinal cord injury occurred at levels adjacent to the osteophytes. Yet, previous experimental studies did not report the presence or location of osteophytes. Considering that cervical disc degeneration has been reported in asymptomatic subjects aged 52 on average (Tao et al., 2021), while they are still active, it is important to study whether osteophytes and spinal degeneration have an impact on neck injury tolerance.

The objective of this study is to characterize injuries and head kinematics resulting from direct dynamic rear head impact as well as the influence of osteophytes on injuries.

2. Methods

2.1 Preparation of post-mortem human subjects

Six male PMHS embalmed with zinc chloride solution (41%) were used (Goodarzi, Akbari and Razeghi Tehrani, 2017). Male subjects were selected since approximately 75% of traumatic spinal cord injury victims are males (Wagnac et al., 2019). The PMHS were aged between 83 and 96 years old, and their height was between 154 and 187 cm. A CT scan was performed to check for spinal pathologies, along with a phantom to enable the measurement of the trabecular bone mineral density (TBMD). Using the 3D slicer software (http://www.slicer.org), the antero-posterior length of the cervical osteophytes was measured as described in Al-Rawahi et al. (2011). The middle sagittal thickness of the cervical spine IVD and the length from C0 to T1 were also measured on the CT images. The facet angles relative to the transversal plane were measured on the CT scan images according to the method described by Ebraheim et al. (2008), and the right and left facet angles were averaged. A Thompson grade for assessing the IVD degeneration was assigned to each subject based on the presence and size of osteophytes (Thompson et al., 1990). The most severe grade among all spinal levels was assigned to each subject.

2.2 Manual mobility evaluation and impact test

Prior to impact, the PMHS were mobilized manually in flexion-extension, axial rotation and lateral bending for 20 cycles to reduce post-mortem rigidity and pre-condition the cervical spine. Then, their

heads were rotated manually to maximal flexion and maximal extension to assess the pre-trauma range of motion (RoM). Position markers were glued on the PMHS head and shoulder. The motion was filmed with two cameras (Fastcam SA3, Photron, San Diego, United States) and the Vic3D system (Correlated Solutions, Irmo, United States) was used to report the markers' 3D positions and measure the head displacements.

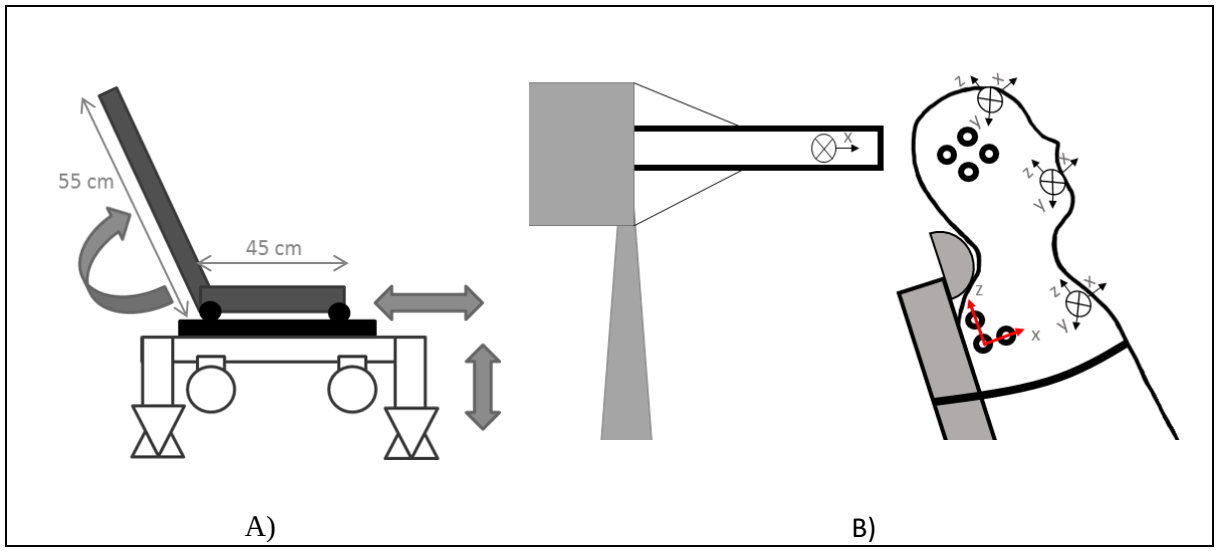

Figure 1 – Test bench and subject instrumentation. A) Seat design and dimensions; grey arrows represent possible seat adjustments. B) Accelerometers and markers' position and coordinate systems. The accelerometers are represented by a black cross. The black and white markers represent the points followed by stereography. The red coordinate system represents the subjects' specific coordinate system.

After the mobility evaluation, head impact was done with a 40 kg horizontal impactor with a cross-section of 75 mm of diameter propelled by a system of springs. A 40 kg mass corresponds approximately to the mass of the head, neck, thorax and arms of a 50th percentile male (De Leva, 1996; Davis, Vavalle and Gayzik, 2015). The dimensions of the impactor were chosen to fit the load cell dimensions (capacity of ±30 kN, type 9347C, Kistler, Winterthur, Switzerland). The PMHS were seated in a custom bench made from an isolated car seat and rails (Peugeot 307, Peugeot, Poissy, France) fixed to an elevation platform (Figure 11). The bench was designed to enable the positioning and orientation of the subject prior to the impact. The seat was adjusted for the impactor to hit the parietal region of the PMHS skull. The parietal region was chosen since it was identified as the main site of impact for rear impact among motorcyclists (Molinero, 2013). The PMHS were attached with straps to the seat: one at the hips and one under the arms. Weights (total of 120 kg) were placed on the platform to reduce its motion during the impact. Four combinations of subject backward inclination, length of contact between the impactor and the head before the impactor is stopped by the propulsors system and velocity of impact were tested, as described in Table 1. The subject backward inclination was measured in the sagittal plane in relation to the erected position and the length of contact was measured by the distance between the head and the end of the impactor trajectory. A backward subject inclination of 25 degrees was chosen to match the inclination of previous PMHS sled tests (Meyer et

al., 2019; Pintar, Yoganandan and Maiman, 2010; White et al., 2009) and to enable impact at the parietal region of the head. The 20 cm length of contact was chosen to ensure full flexion of the neck. The impact energy was measured as half of the mass multiplied by the velocity square (Schmitt et al., 2019). Three impact velocities (3.5, 4.7 and 5.5 m/s) were chosen to fit past experimental testing (Nightingale et al., 1996; Saari, Itshayek and Cripton, 2011; Ivancic, 2012; Viano and Parenteau, 2008; N. A. Yoganandan et al., 2000) and to surpass the neck injury tolerance. A 2 cm thick foam protector (PUG-10-480) was placed at the extremity of the impactor. A helmet (Oxelo MF500, Decathlon, Lille, France) was used at medium and high velocity to avoid skull fracture (identified in Table 1). A flexible plastic was positioned to support the back of the neck and maintain C4-C5 perpendicular to the seat, which ensured a neutral positioning of the neck (Saari, Itshayek and Cripton, 2011). After impact, the manual mobility evaluation procedure was repeated.

Table 1 – Impact conditions

Subject number	**Impact velocity (m/s)**	**Impact energy (J)**	**Head backward angle (degrees)**	**Length of contact between the head and impactor (cm)**	**Helmet used**
1	3.5	245	25	0	No
2	3.5	259	0	20	No
3	4.7	461	25	20	Yes
4	4.7	442	25	20	Yes
5	5.5	627	25	20	Yes
6	5.5	605	25	20	Yes

2.3 Instrumentation and data analysis

The PMHS were equipped with nine ±250 g range uniaxial accelerometers (EGAS S403A-250-/L1.5M, TE Connectivity, Schaffhouse, Switzerland): 3 on the forehead, 3 in the mouth and 3 on the sternum. One uniaxial accelerometer was placed on the impactor in the direction of the impact. The location and coordinate systems of the accelerometers are shown in Figure 1. A triaxial load cell (capacity of ±30 kN, type 9347C, Kistler, Winterthur, Switzerland) was placed on the impactor under the foam protector. Data were collected at 10 000 Hz by the data acquisition system (Kidau 3446, Kistler, Winterthur, Switzerland).

Acceleration and force data were filtered using a low-pass second-order Butterworth filter (cut-off frequency of 1000 Hz) as recommended by the SAE J211 specifications. The resultant of the mouth accelerometer data in the three axes was reported since it is difficult to correctly align the accelerometers in the mouth. The head and shoulder markers' 3D positions were recorded using Vic3D. The images were filmed at 1000 Hz with two high-speed cameras (Fastcam SA3, Photron, San Diego, United States). The subject-specific coordinate system (SCS) was constructed from three markers placed on the subject (Figure 1). The markers' positions were then projected onto the SCS sagittal plane to measure the head rotation and displacements during mobility evaluation and impact testing. The timing of the head rotation relative to the head anterior translation was measured using the head displacement data.

After the impact and post-trauma manual mobility evaluation, another CT scan was performed. The images were reviewed by a neurosurgeon to identify bony fractures and signs of disco-ligamentous injuries. Finally, the cervical spine was dissected by a neurosurgeon. The integrity of the IVD and ligaments was visually assessed. The AO spine classifications for the upper cervical spine (C0-C3) and subaxial spine were used to classify the injuries (Vaccaro et al., 2016; Divi et al., 2019).

3. Results

Table 2 shows the anterior osteophytes' spinal level, type of osteophytes, antero-posterior length and volume. The PMHS' age, measured TBMD, the IVD middle thickness and the Thompson grade are also presented in Table 2. The average TBMD was between 200 mg/cc and 370 mg/cc and the Thompson grade between III and V. Two subjects (PMHS #1 and #5) had no anterior vertebral osteophytes. PMHS #2 was the most osteoarthritic, with the lowest TBMD. The anterior osteophytes were fused at C4-C5 and the vertebrae C6 and C7 were fused.

Table 2 – Trabecular bone density, anterior osteophytes description and intervertebral disc average middle height and subject age

Subject number	**Age**	**Trabecular bone mineral density (mg/cc)**	**Antero-posterior length of osteophytes (mm)**	**Intervertebral disc thickness (mm)**	**Facet angle relative to transverse plane (degrees)**	**Most severe Thompson grade**
1	83	C2: 330 C3: 370 C4: 400 C5: 430 C6: 350 C7: 310 **Average**: 370	0	C2-C3: 5.3 C3-C4: 4 C4-C5: 3.5 C5-C6: 1.2 C6-C7: 4.1 C7-T1: 3.8 **Average: 3.7**	C2-C3: 67 C3-C4: 51 C4-C5: 41 C5-C6: 35 C6-C7: 25 C7-T1: 13	III
2	94	C2: 230 C3: 240 C4: 230 C5: 170 C6: 170 C7: 190 **Average**: 200	C2: 10 C3: 6.4 C4: 5.9 C5: 5.1	C2-C3: 4.1 C3-C4: 2.7 C4-C5: 2.8 C5-C6: 3 C6-C7: 0 (fused vertebrae) C7-T1: 4.5 **Average: 2.9**	C2-C3: 38 C3-C4: 38 C4-C5: 27 C5-C6: 24 C6-C7: 28 C7-T1: 15	V
3	84	C2: 320 C3: 310 C4: 390 C5: 420 C6: 370 C7: 340 **Average**: 360	C4: 4.5 C5: 3.7 C6: 2.3	C2-C3: 5 C3-C4: 4.6 C4-C5: 2.8 C5-C6: 2.6 C6-C7: 4.7 C7-T1: 4.1 **Average: 4**	C2-C3: 55 C3-C4: 37 C4-C5: 28 C5-C6: 14 C6-C7: 11 C7-T1: 6	V
4	82	C2: 310 C3: 350 C4: 350 C5: 350 C6: 310 C7: 300 **Average**: 330	C5: 1.3 C6: 1.8	C2-C3: 3.6 C3-C4: 4.3 C4-C5: 4.3 C5-C6: 3 C6-C7: 4.1 C7-T1: 3.7 **Average : 3.8**	C2-C3: 37 C3-C4: 41 C4-C5: 35 C5-C6: 29 C6-C7: 26 C7-T1: 17	IV
5	88	C2: 300 C3: 300 C4: 380 C5: 400 C6: 320 C7: 280 **Average**: 330	0	C2-C3: 4.3 C3-C4: 2.8 C4-C5: 3.4 C5-C6: 3.5 C6-C7: 2.4 C7-T1: 4 **Average: 3.4**	C2-C3: 49 C3-C4: 37 C4-C5: 25 C5-C6: 18 C6-C7: 14 C7-T1: 6	III
6	96	C2: 380 C3: 330 C4: 230 C5: 180 C6: 190 C7: 290 **Average**: 270	C4: 2.5 C5: 2.5 C6: 3	C2-C3: 3.9 C3-C4: 2.7 C4-C5: 2.4 C5-C6: 1.7 C6-C7: 2.1 C7-T1: 2.2 **Average: 2.5**	C2-C3: 57 C3-C4: 51 C4-C5: 30 C5-C6: 29 C6-C7: 31 C7-T1: 23	V

Different injuries were identified on the post-impact CT scan images and during dissection (Figure 2). A schematic representation of the subjects' cervical spine, the post-trauma injuries and the anterior osteophytes are reported in Figure 3. The two PMHS without anterior osteophytes (PMHS #1 and #5) had fractures at the C2 vertebral body (**Erreur ! Source du renvoi introuvable.** 3). PMHS #2 presented a fracture of the superior osteophyte at C3 and a fracture at the fused C6-C7 vertebrae. The other three subjects (#3, #4 and #6) had posterior disco-ligamentous injuries at C6-C7 or C7-T1 (type B2). The other injuries were fractures at the facets at C3-C4, C5-C6 or C6-C7 (type F1). PMHS #6 also had fractures of the lamina at C3 and of the lamina and spinous process at C6. There was one case of subluxation at C1-C2 (PMHS #5).

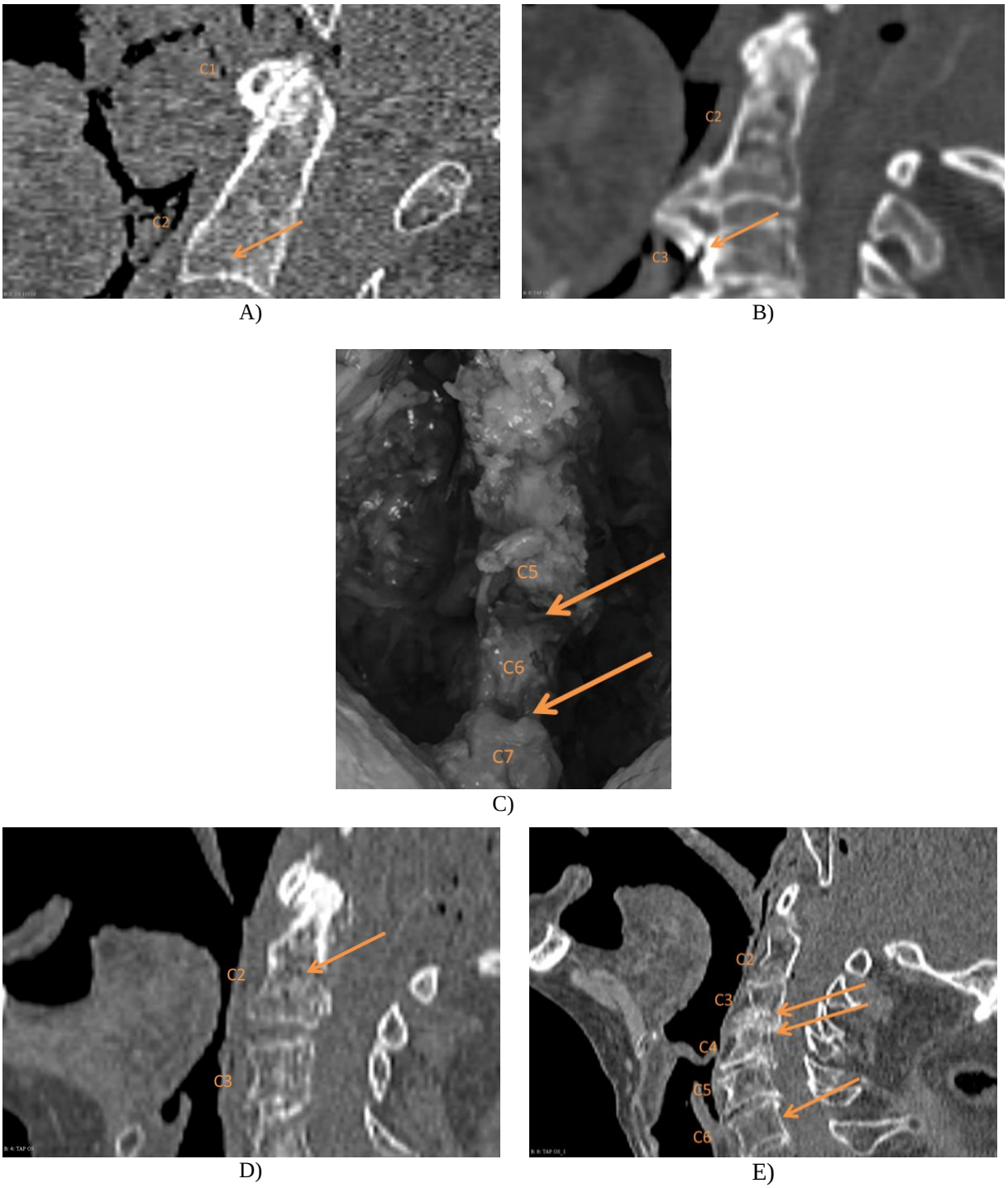

Figure 2 – Post-impact injuries as seen on CT scan images. A) C2 endplate fracture shown on CT scan images (PMHS #1) B) Anterior osteophyte fracture at C3 shown on CT scan images (PMHS #2) C) Dissection of posterior cervical spine showing ligamentous disruption at C5-C6 and C6-C7 (PMHS #4) D) Odontoid fracture shown on CT scan images (PMHS #5) E) Vertebral body fracture at C3, C4 and C6 shown on CT scan images (PMHS #6)

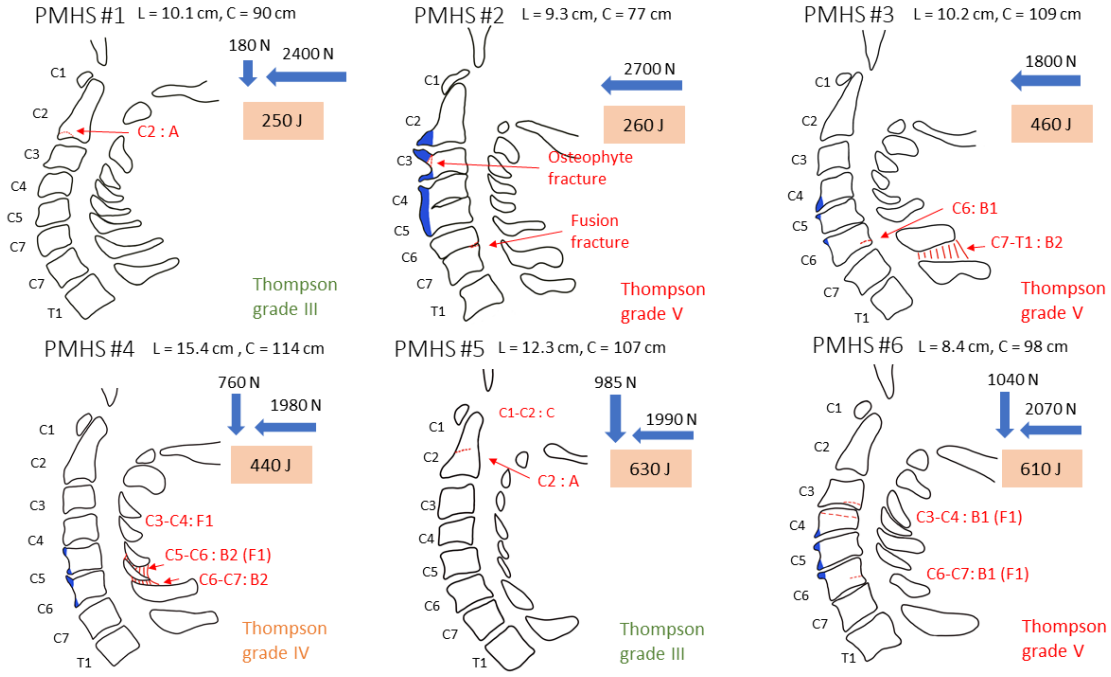

Figure 3 – Cervical spine contour of the subject after the impact. Schematic representation made from CT images of the subjects and post-trauma dissection. Osteophytes are represented in blue, fractures are represented by dotted red lines and disco-ligamentous injuries are represented by red dashes. L is the length of the neck from C0 to T1. C is the circumference of the neck, including the soft tissues. The Thompson grade corresponds to the most severe grade in the entire cervical spine. The impact force in the axial and antero-posterior direction is given in Newton adjacent to the blue arrows and the energy of the impact is indicated in joules in the orange square.

The head flexion-extension RoM measured during the manual mobility tests before and after the impact are presented in Table 3. This test was not performed on PMHS #1 and #2. The flexion-extension RoM increased between 35 and 75% after impact. The PMHS with larger osteophytes had a smaller pre-impact global RoM. The head displacements relative to the shoulders during the impact are presented in Table 3. The cranial-caudal displacements were between -12 and -196 mm. In all cases, the cranial-caudal displacement was negative, which is normal during neck flexion. This movement was generally larger as the impact velocity increased. The relative anterior posterior translation (90 to 140 mm), however, did not show a relation with the impact velocity. Finally, the head rotation was almost doubled from the lowest velocity (43 to 45 degrees) to the medium and high velocity (between 69 and 78 degrees). The head anterior translation occurred prior to head rotation in all cases and with a delay of 14 ms on average.

Table 3 – Pre- and post-trauma flexion-extension global range of motion and head displacements during impact relative to the shoulders measured by markers tracking

Subject number	Pre-impact flexion-extension RoM (degrees)	Post-impact flexion-extension RoM (degrees)	Difference between the pre- and post-impact RoM (%)	Head cranial-caudal displacement during impact (mm)	Head antero-posterior displacement during impact (mm)	Head rotation during impact (degrees)	Timing head rotation relative to head translation (ms)
1				-12.1	90.4	43	13
2				-30.1	139.3	45	15
3	32	56	75	-97.6	125.5 *	78	6
4	34	50	47	-195.6	118.8	75	10
5	57	77	35	-194.7 *	133.3 *	71	16
6	42	66	57	-182.7	98.2	69	23

Asterisks indicates that some of the test data are missing due to a loss of visualization of markers.

The load cell data for all the impacts in the antero-posterior and cranial-caudal directions are presented in Figure 4. The antero-posterior direction force was higher for PMHS #1 and #2 because of the absence of a helmet, and the duration of the impact was about 3 times smaller. From the medium velocity impacts (PMHS #3 and #4) to the high velocity impacts (PMHS #5 and #6), the antero-posterior force increased slightly (8%), and the shape of the curves were similar. The axial force increased between the three velocities. There was a positive force measured in the axial direction for subject #3, which may have been caused by a slippage of the impactor on the helmet. There was a dip in the antero-posterior curve for PMHS #4, accompanied by a rise in the axial force, which could also be explained by a slippage of the impactor.

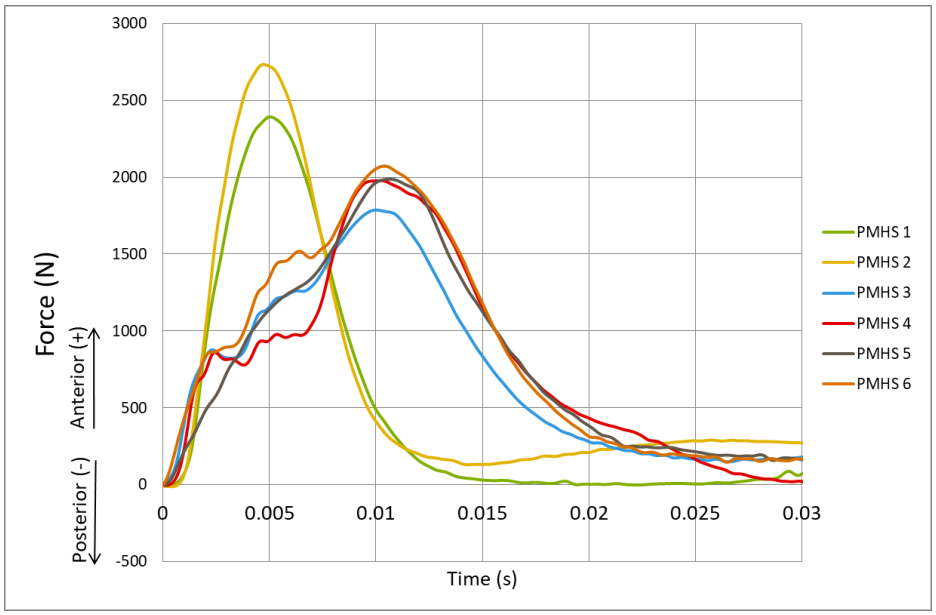

A)

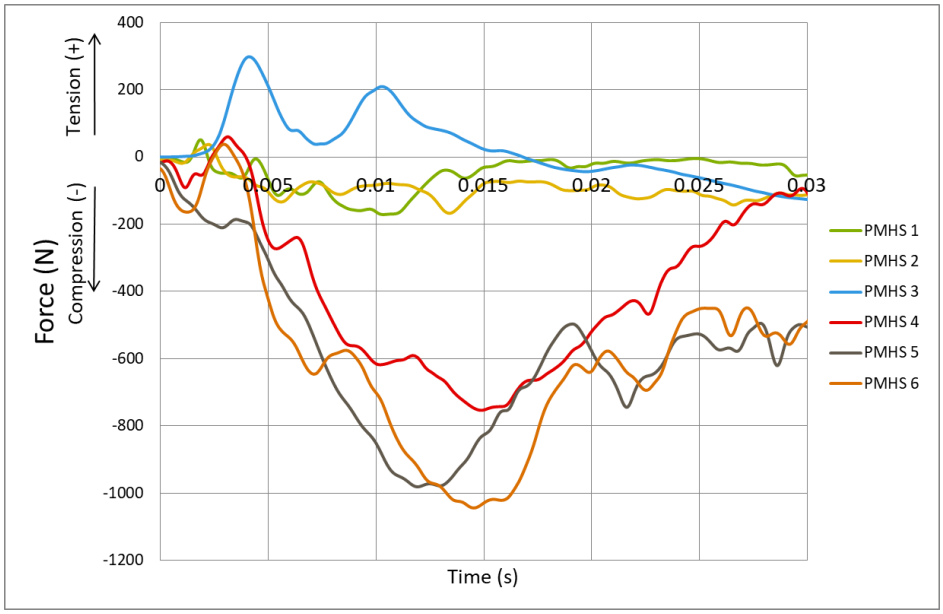

B)

Figure 4 – Load cell data at the impactor in A) the antero-posterior direction and B) the cranial-caudal direction. Forces (Newtons) measured during the impact for PMHS 1 to 6 in relation to time (seconds). The data were filtered with a low-bass second-order Butterworth filter. The triaxial cell load was placed on the impactor under the protective foam.

Peak values of the PMHS accelerometers data are shown in Table 4. Peak accelerations in the left-right direction (y) were small as compared to the other accelerations, which show that the motion was mostly in the sagittal plane. The sternum accelerations magnitudes were 13 to 55% of the forehead resultant accelerations, indicating that the sternum motion was still present. The resultant acceleration

measured at the mouth was between 55 and 147 g, and tended to increase with the velocity of the impactor. Some accelerometers data are absent for PMHS #5 and #6 due to material malfunction.

Table 4 – Peak accelerations during the impact for all the PMHS

Subject number	**Forehead acceleration (X) (g)**	**Forehead acceleration (Y) (g)**	**Forehead acceleration (Z) (g)**	**Sternum acceleration (X) (g)**	**Sternum acceleration (Y) (g)**	**Sternum acceleration (Z) (g)**	**Mouth resultant acceleration (g)**
1	39	-9	55	31	2	8	55
2	47	-5	0	5	-2	10	69
3	30	-7	-78	-4	-1	-10	83
4	97	29	-163	-91	-1	8	147
5	ERROR	ERROR	ERROR	-64	2	-13	ERROR
6	14	-13	-108	59	-3	-12	ERROR

4. Discussion

This, to our knowledge, is the first full scale study to test rear head impact on PMHS. A new test bench and protocol were designed to submit six male PMHS to a rear head impact of 250 to 630 joules. Using whole body PMHS generates less artificial boundary conditions as compared to head-neck specimens, whose fixation leads to high loads at the lower segments. The rigidity due to soft tissues and passive muscles is also preserved. These factors lead to more realistic impact loads, head kinematics and injury patterns. This study provides essential information allowing to understand the dynamic head impact and to validate finite elements models that simulate dynamic neck loading. This is also the first experimental study to investigate the impact of osteophytes on cervical spine injuries.

Most of the injuries produced herein were flexion-distraction type injuries (type B1 or B2 in the AOSpine classification) and two PMHS had an articular facet fracture. Posterior disco-ligamentous injuries were confirmed at autopsy at C5-C6 (once) and C6-C7 (twice). C6-C7 was the most commonly injured level. This corresponds to the most frequent spinal levels for clinical flexion-distraction injuries at the cervical spine (Quarrington et al., 2018). The prevalence of disco-ligamentous injuries at the subaxial cervical spine (C5-C7) suggests that these injuries are created by

tensile loading of the posterior elements. The flexion moment in the cervical spine created by the antero-posterior impact force is higher in the lower cervical spine due to the longer moment arm. The facets' angles relative to the transversal plane at the subaxial cervical spine are smaller (24 degrees on average at C5-C6 and C6-C7 for our subjects), which means that the articular facets can offer less resistance against anterior shear as compared to the cranial levels, which could explain the prevalence of injuries at C6-C7. Two subjects suffered from C2 fracture and one (PMHS #5) also had a C1-C2 subluxation. C2 fracture due to falls or motor vehicle accidents are frequent in older patients (Tadros et al., 2019; Barrey et al., 2021). While odontoid fracture has been associated with upper cervical spine hyper-extension (Ivancic, 2014), in vitro testing has suggested that the odontoid process is prone to avulsion from tensile forces due to extension or flexion of the upper cervical spine (Nightingale et al., 2002; 2007). Althoff (1979) showed that a combination of antero-posterior shear (both in anterior and in posterior) and axial compression lead to odontoid fractures, while hyper-flexion, hyper-extension or shear loading only did not. This is similar to what we observed for PMHS #5, and suggests that anterior shearing and compression is a possible injury mechanism for odontoid process fracture.

Two of the PMHS suffered from injuries at non-contiguous spinal levels, which is similar to Ivancic (2012), who observed neck buckling causing injuries to the posterior ligaments at C7-T1, accompanied by injuries at another FSU at the upper or middle spine. They also reported spinous process fractures and atlas and odontoid fractures, similarly to our study. However, their specimens were osteo-ligamentous cervical spines combined with an artificial head, and the impact was performed on the top of the skull. Pintar et al. (2010) obtained dislocations at C6-C7 or C7-T1, accompanied by vertebral body fracture on three specimens during frontal sled tests. However, their impact velocities, 6.9 m/s and 15.8 m/s, were superior to our velocities, and they used a multi-impact protocol. Pintar et al. (1998) obtained cases of posterior ligament disruption at the lower cervical spine and cases of vertebral fractures or dislocations. However, they applied a vertical load at 2 to 5 m/s on the head with the cervical spine pre-flexed, while our PMHS had a neutral cervical spine position and were impacted at the rear of the head. Their measured failure forces ranged from 3000 to 9700 N, which is higher than the loads we measured: resultant force of 1800 N to 2800 N at the impactor. In the present study, the maximum forces were similar in amplitude to the force at the impact surface reported by Nightingale et al. (1996), even though the muscles were removed from their specimens. The axial compression force was small as compared to the anteroposterior force for PMHS #1 to 3. In subjects #4 to 6, the compressive force represented 40 to 50% of the anteroposterior force, which might have contributed to the creation of facet fractures (PMHS #4 and #6). Our experimental results show that anterior shear and flexion loading of the spine can lead to flexion-distraction injuries. However, a greater compressive force may be needed to result in subluxation or dislocation, which could be tested in a future study.

Distinct injury patterns were observed depending on the presence and location of anterior vertebral osteophytes. The specimens without anterior osteophytes suffered from C2 vertebral body fracture. The subjects with anterior osteophytes did not have injuries at the upper cervical spine, but B1 or B2 injury at the subaxial spine. This suggests that the presence of anterior vertebral osteophytes protected the osteoarthritic subjects from upper cervical spine injury. Osteophytes were found to resist bending moments at the thoracolumbar spine (Al-Rawahi et al., 2011) and to reduce cervical RoM (Kuhlman, 1993). FSU with osteophytes offer better resistance to axial loading and are less prone to compression fracture (Wagnac et al., 2017). Therefore, anterior osteophytes and lower bone density seem to protect the PMHS from the occurrence of bone fracture. The pre-trauma RoM of PMHS #3 and #4 (with anterior osteophytes) was smaller than the pre-trauma RoM of PMHS #5, with no anterior vertebral osteophyte. This is in agreement with established knowledge that RoM decreases with age and with the presence of osteophytes at the thoracic spine (Healy et al., 2015). Pre-impact RoM in flexion-extension showed that subjects with more osteophytes had a smaller initial RoM. Therefore, anterior osteophytes seem to limit the bending of the spine. Also, the osteophyte fracture at C3 observed for PMHS #2 suggests that the osteophytes resisted movement during the impact. However, our results also show that B1 type fractures were produced at levels inferior or superior to osteophytic bridges. The same phenomenon was observed by Sasaki et al. (2018) for cervical spine injuries in professional wrestlers with giant anterior osteophytes. Our experimental results suggest that anterior osteophytes provide stability in flexion and protect the spinal levels where they are formed but seem to increase the stress at the adjacent spinal levels. However, given the small number of subjects in our study and the absence of a control group without spinal degeneration, the observed trends should be confirmed through additional experiments. Finite element analysis could investigate the impact of spinal degeneration by controlling the number, size and position of anterior osteophytes and the rigidity of the cervical spine and the bone quality. The clinical care of patients with an osteophyte fracture should include observation of the state of the osteophytes, and immobilization could be recommended until the osteophytes have been repaired. Also, active patients with diagnosed osteophytes should be advised of the potentially increased risk of injury.

In our study, the forehead and mouth acceleration were higher than the head acceleration previously reported at the head center of gravity in full scale experiments using sled tests (N. A. Yoganandan et al., 2000; Pintar, Yoganandan and Maiman, 2010). However, the head accelerations are in concordance with what was reported at the head center of gravity for direct head impact on PMHS by Viano and Parenteau (2008). Head acceleration increased with impact velocity, but for the tested range, it did not seem to increase the risk of injury. Cranial-caudal displacement increased with the velocity of the impact and head rotation, but the maximum antero-posterior displacement showed no clear pattern. The amplitude of antero-posterior displacement is probably dependent on the subject's

morphometry, but may also be influenced by other spine motions, such as cervical spine buckling. For every subject, head rotation occurred after head anterior translation, with a delay of 6 to 23 ms, indicating the importance of anterior shear as compared to flexion in the injury mechanism. Global head rotation increased from low velocity to medium and high velocities, but not between the medium and high velocities. Neck rotation exceeded the physiological maximum flexion of 65° determined by Niewiadomski et al. (2019) and the maximum flexion of 48.5° determined for volunteers wearing a motorcycle helmet (Lecoublet et al., 2019) for PMHS hit at medium and high velocities (# 3 to 6), but not for PMHS hit at low velocity. The same protocol should be applied in the future to PMHS equipped with a motorcycle helmet or a neck brace since wearing protective equipment affects the head kinematics, and therefore, the resultant injuries. Articular facet fracture and disco-ligamentous injuries were seen only for cases of high flexion, suggesting that flexion is an important mechanism in the development of this type of injury.

This study has certain limitations that should be noted. The subjects were older than the average age for traumatic spinal cord injury (Wagnac et al., 2019), and some had important anterior osteophytes and grade IV or V degeneration (Thompson et al., 1990). However, osteoarthritis frequently develops with age (Anderson and Loeser, 2010). Considering that the osteoarthritic cervical spine has a different biomechanical behaviour than the healthy spine and that the number of older drivers is increasing (Islam and Mannering, 2006), it is essential to improve our knowledge of the osteoarthrosis cervical spine response to dynamic loading and tolerance to injury. Furthermore, age is related to decreasing RoM, decreasing IVD height and decreasing anteroposterior spinal canal width at the cervical spine (Yukawa et al., 2012). These phenomena are susceptible to impact the cervical injury response, and older people have been shown to be at greater risk of spinal injury in motor vehicle accidents (Bilston, Clarke, and Brown, 2011). Finite element analysis could be performed in a future study to investigate the impact of cervical spine degeneration due to age on the pattern of injuries and tolerance to injury. Only male subjects were used in the present study since traumatic spinal cord injury is more frequent in men (Wagnac et al., 2019). Considering the anatomical differences between men and women (Linder and Svedberg, 2019; N. Yoganandan et al., 2017), the head kinematics and the injury patterns reported herein are likely to differ with gender. Further experiments should include female subjects to investigate these differences. Indeed, previous studies have shown different head and neck kinematic responses between male and female subjects (Siegmund et al., 1997; Stemper, Yoganandan, and Pintar, 2003; Linder and Svedberg, 2019) and greater intervertebral angles under dynamic loading in female head-neck specimens (Stemper, Yoganandan, and Pintar, 2003). Moreover, attaching subjects to the seat may lead to unrealistic movements between the torso and the neck and reduce the likelihood of neck buckling due to torso inertia. This might therefore affect the cervical spine injury response. However, this effect appears less significant than the boundary conditions

created by fixation at the bottom of the cervical spine done with head-neck specimens. While the muscles were preserved, the effect of muscle activation is absent in this experiment. However, for severe impacts, muscle activation during head impact is negligible as compared to the effect of ligaments and passive muscles (Kuo et al., 2019). Finally, the number of subjects was too small to allow a statistical analysis of the test parameters' effect, which is often the case with full body cadaveric studies. More tests should be done in the future to better understand the effects of the impact velocity and the PMHS morphology and bone pathology.

5. Conclusions

Understanding the mechanisms of injury and neck tolerance is fundamental in the design of protective devices. Clinically relevant injuries were obtained by applying dynamic rear head impacts at 3.5 to 5.5 m/s on PMHS. The injuries sustained demonstrate that rear head impact and anteroposterior shear and flexion neck loading can lead to flexion-distraction injuries, falling under types B1 and B2 of the AO Spine classification. A novel experimental protocol was designed and can be used to investigate the effectiveness of protective devices in the context of direct head impact. Significant anterior vertebral osteophytes appear to protect the specimens from injury by limiting the neck flexion, but also lead to stress concentration at the level adjacent to the osteophytes. Clinical care of older patients who have sustained a cervical spine injury should incorporate a close follow-up of the osteophyte state. If an osteophyte fracture is noted, immobilization should be recommended until the fusion of the osteophyte.

Conflict of interest

The authors have no conflict of interest to report regarding this study.

Acknowledgments

The authors would like to thank Virginie Bascop, Max Py and Catherine Masson for their participation in the experiments. This research was funded by the Federation Internationale de l'Automobile; the Canada Research Chair in Biomechanics of Head and Spine Injuries [grant number 231815]; and the Fonds de recherche du Québec [grant number 271503]. The funding sources were not involved in the study design or writing of the paper. This study was approved by École de technologie supérieure, Montréal, Canada under reference number H20180509.

CRediT authorship contribution statement

Marie-Hélène Beauséjour: Conceptualization, Methodology, Investigation, Writing – Original Draft. **Yvan Petit:** Conceptualization, Supervision, Writing – Review & Editing. **Éric Wagnac:** Conceptualization, Writing – Review & Editing. **Anthony Melot:** Conceptualization, Investigation, Writing – Review & Editing. **Lucas Troude:** Conceptualization, Investigation, Writing – Review & Editing. **Pierre-Jean Arnoux:** Conceptualization, Resources, Writing – Review & Editing, Supervision, Project administration, Funding acquisition.

Bibliography

Al-Rawahi, Maimouna, Jin Luo, Phillip Pollintine, Patricia Dolan, and Michael A Adams. 2011. "Mechanical function of vertebral body osteophytes, as revealed by experiments on cadaveric spines". *Spine* 36 (10): 770-77.

Althoff, B and P Bardholm. 1979. "Fracture of the odontoid process. A clinical and radiographic study". *Acta Orthop Scand Suppl* 177: 61-95.

Anderson, Shane A. and Richard F. Loeser. 2010. "Why is osteoarthritis an age-related disease?" *Osteoarthritis* 24 (1): 15-26. https://doi.org/10.1016/j.berh.2009.08.006.

Bailly, Nicolas, Maxime Llari, Thierry Donnadieu, Catherine Masson, and Pierre-Jean Arnoux. 2018. "Numerical Reconstruction of Traumatic Brain Injury in Skiing and Snowboarding." *Medicine and science in sports and exercise* 50 (11): 2322-29.

Barrey, C. Y., A. di Bartolomeo, L. Barresi, N. Bronsard, J. Allia, B. Blondel, S. Fuentes, et al. 2021. "C1-C2 Injury: Factors influencing mortality, outcome, and fracture healing". *European Spine Journal*, February. https://doi.org/10.1007/s00586-021-06763-x.

Bilston, Lynne E, Elizabeth C Clarke, and Julie Brown. 2011. "Spinal injury in car crashes: crash factors and the effects of occupant age". *Injury Prevention* 17 (4): 228-32.

Blauth, MKA, G Mair, R Schmid, M Reinhold, and M Rieger. 2007. "Classification of injuries of the subaxial cervical spine". *AO spine manual: clinical applications. Thieme, Stuttgart*, 21-38.

Bourdet, Nicolas, Caroline Deck, Thierry Serre, Christophe Perrin, Maxime Llari, and Rémy Willinger. 2014. "In-depth real-world bicycle accident reconstructions". *International journal of crashworthiness* 19 (3): 222-32.

Davis, Matthew L, Nicholas A Vavalle, and F Scott Gayzik. 2015. "An evaluation of mass-normalization using 50th and 95th percentile human body finite element models in frontal crash". In , 608-21.

De Leva, Paolo. 1996. "Adjustments to Zatsiorsky-Seluyanov's segment inertia parameters". *Journal of biomechanics* 29 (9): 1223-30.

Dennison, Christopher R, Erin M Macri, and Peter A Cripton. 2012. "Mechanisms of cervical spine injury in rugby union: is it premature to abandon hyperflexion as the main mechanism underpinning injury?"

Divi, Srikanth N, Gregory D Schroeder, F Cumhur Oner, Frank Kandziora, Klaus J Schnake, Marcel F Dvorak, Lorin M Benneker, Jens R Chapman, and Alexander R Vaccaro. 2019. "AOSpine—Spine Trauma Classification System: The Value of Modifiers: A Narrative Review With Commentary on Evolving Descriptive Principles". *Global spine journal* 9 (1_suppl): 77S-88S.

Ebraheim, Nabil A, Vishwas Patil, Jiayong Liu, Steve P Haman, and Richard A Yeasting. 2008. "Morphometric analyses of the cervical superior facets and implications for facet dislocation". *International orthopaedics* 32 (1): 97-101.

Goodarzi, Nader, Ghasem Akbari, and Payam Razeghi Tehrani. 2017. "Zinc chloride, a new material for embalming and preservation of the anatomical specimens". *Anatomical Sciences Journal* 14 (1): 25-30.

Healy, Andrew T, Prasath Mageswaran, Daniel Lubelski, Benjamin P Rosenbaum, Virgilio Matheus, Edward C Benzel, and Thomas E Mroz. 2015. "Thoracic range of motion, stability, and correlation to imaging-determined degeneration". *Journal of Neurosurgery: Spine* 23 (2): 170-77.

Islam, Samantha and Fred Mannering. 2006. "Driver aging and its effect on male and female single-vehicle accident injuries: Some additional evidence". *Journal of Safety Research* 37 (3): 267-76. https://doi.org/10.1016/j.jsr.2006.04.003.

Ivancic, Paul C. 2012. "Head-First Impact With Head Protrusion Causes Noncontiguous Injuries of the Cadaveric Cervical Spine". *Clinical Journal of Sport Medicine* 22 (5). https://journals.lww.com/cjsportsmed/Fulltext/2012/09000/Head_First_Impact_With_Head_Protrusion_Causes.3.aspx.

Ivancic, Paul C. 2014. "Odontoid fracture biomechanics". *Spine* 39 (24): E1403-10.

Izzo, Roberto, Teresa Popolizio, Rosario Francesco Balzano, Anna Maria Pennelli, Anna Simeone, and Mario Muto. 2019. "Imaging of cervical spine traumas". *European journal of radiology*.

King, Albert I. 2018. *The biomechanics of impact injury*. Springer.
Kuhlman, Kurt A. 1993. "Cervical range of motion in the elderly". *Archives of physical medicine and rehabilitation* 74 (10): 1071-79.
Kuo, Calvin, Jodie Sheffels, Michael Fanton, Ina Bianca Yu, Rosa Hamalainen, and David Camarillo. 2019. "Passive cervical spine ligaments provide stability during head impacts". *Journal of the Royal Society Interface* 16 (154): 20190086.
Lecoublet, Brieg, Dominic Boisclair, Morgane Evin, Eric Wagnac, Yvan Petit, Carl-Eric Aubin, and Pierre-Jean Arnoux. 2019. "Assessing the global range of motion of the helmeted head through rotational and translational measurements". *International journal of crashworthiness*.
Linder, Astrid and Wanna Svedberg. 2019. "Review of average sized male and female occupant models in European regulatory safety assessment tests and European laws: Gaps and bridging suggestions". *Accident Analysis & Prevention* 127: 156-62.
Maiman, Dennis J., Narayan Yoganandan, and Frank A. Pintar. 2002. "Preinjury cervical alignment affecting spinal trauma". *Journal of Neurosurgery: Spine* 97 (1). https://thejns.org/spine/view/journals/j-neurosurg-spine/97/1/article-p57.xml.
Mattucci, Stephen, Jason Speidel, Jie Liu, Brian K Kwon, Wolfram Tetzlaff, and Thomas R Oxland. 2019. "Basic biomechanics of spinal cord injury—How injuries happen in people and how animal models have informed our understanding". *Clinical biomechanics* 64: 58-68.
Meyer, Frank, John Humm, Yuvaraj Purushothaman, Rémy Willinger, Frank A Pintar, and Narayan Yoganandan. 2019. "Forces and moments in cervical spinal column segments in frontal impacts using finite element modeling and human cadaver tests". *Journal of the mechanical behavior of biomedical materials* 90: 681-88.
Molinero, A. 2013. *Motorcyclists road safety improvement through better performance of the protective equipment and first aid devices*.
Niewiadomski, Céline, Rohan-Jean Bianco, Sanae Afquir, Morgane Evin, and Pierre-Jean Arnoux. 2019. "Experimental assessment of cervical ranges of motion and compensatory strategies". *Chiropractic & Manual Therapies* 27 (1): 9.
Nightingale, Roger W, Cameron R Bass, and Barry S Myers. 2019. "On the relative importance of bending and compression in cervical spine bilateral facet dislocation". *Clinical Biomechanics* 64: 90-97.
Nightingale, Roger W, V Carol Chancey, Danielle Ottaviano, Jason F Luck, Laura Tran, Michael Prange, and Barry S Myers. 2007. "Flexion and extension structural properties and strengths for male cervical spine segments". *Journal of biomechanics* 40 (3): 535-42.
Nightingale, Roger W, James H McElhaney, William J Richardson, Thomas M Best, and Barry S Myers. 1996. "Experimental impact injury to the cervical spine: relating motion of the head and the mechanism of injury". *JBJS* 78 (3): 412-21.
Nightingale, Roger W, Beth A Winkelstein, Kurt E Knaub, William J Richardson, Jason F Luck, and Barry S Myers. 2002. "Comparative strengths and structural properties of the upper and lower cervical spine in flexion and extension". *Journal of biomechanics* 35 (6): 725-32.
Pintar, Frank A., Sances Anthony, Narayan Yoganandan, John Reinartz, Dennis J. Maiman, Jung Keun Suh, George Unger, Joseph F. Cusick, and Sanford J. Larson. 1990. "Biodynamics of the Total Human Cadaveric Cervical Spine". In . SAE International. https://doi.org/10.4271/902309.
Pintar, Frank A., L.m. Voo, Narayan A. Yoganandan, T.h. Cho, and D.J. Maiman. 1998. "Mechanisms of Hyperflexion Cervical Spine Injury". *Proceedings of the International Research Council on the Biomechanics of Injury Conference* 26: 249-60.
Pintar, Frank A., Narayan Yoganandan, and Dennis J. Maiman. 2010. "Lower Cervical Spine Loading in Frontal Sled Tests Using Inverse Dynamics: Potential Applications for Lower Neck Injury Criteria". In . The Stapp Association. https://doi.org/10.4271/2010-22-0008.
Quarrington, Ryan D, Claire F Jones, Petar Tcherveniakov, Jillian M Clark, Simon JI Sandler, Yu Chao Lee, Shabnam Torabiardakani, John J Costi, and Brian JC Freeman. 2018. "Traumatic subaxial cervical facet subluxation and dislocation: epidemiology, radiographic analyses, and risk factors for spinal cord injury". *The Spine Journal* 18 (3): 387-98.
Saari, A, E Itshayek, and Peter A Cripton. 2011. "Cervical spinal cord deformation during simulated head-first impact injuries". *Journal of biomechanics* 44 (14): 2565-71.

Sasaki, Manabu, Shunji Asamoto, Masao Umegaki, and Katsumi Matsumoto. 2018. “Cervical osteogenic degeneration in Japanese professional wrestlers and its relationship to cervical spine injury”. *Journal of Neurosurgery: Spine* 29 (6): 622-27.

Schmitt, Kai-Uwe, Peter F Niederer, Duane S Cronin, Barclay Morrison III, Markus H Muser, and Felix Walz. 2019. *Trauma biomechanics: an introduction to injury biomechanics*. Springer.

Siegmund, Gunter P, David J King, Jonathan M Lawrence, Jeffrey B Wheeler, John R Brault, and Terry A Smith. 1997. “Head/neck kinematic response of human subjects in low-speed rear-end collisions”. *SAE transactions*, 3877-3905.

Stemper, Brian D, Narayan Yoganandan, and Frank A Pintar. 2003. “Gender dependent cervical spine segmental kinematics during whiplash”. *Journal of biomechanics* 36 (9): 1281-89.

Tadros, Allison, Melinda Sharon, Kristen Craig, and William Krantz. 2019. “Characteristics and Management of Emergency Department Patients Presenting with C2 Cervical Spine Fractures”. Edited by William B. Rodgers. *BioMed Research International* 2019 (May): 4301051. https://doi.org/10.1155/2019/4301051.

Tao, Youping, Fabio Galbusera, Frank Niemeyer, Dino Samartzis, Daniel Vogele, and Hans-Joachim Wilke. 2021. “Radiographic cervical spine degenerative findings: a study on a large population from age 18 to 97 years”. *European Spine Journal* 30 (2): 431-43.

Thompson, JP, RH Pearce, MT Schechter, ME Adams, IKY Tsang, and PB Bishop. 1990. “Preliminary evaluation of a scheme for grading the gross morphology of the human intervertebral disc”. *Spine* 15 (5): 411-15.

Vaccaro, Alexander R, John D Koerner, Kris E Radcliff, F Cumhur Oner, Maximilian Reinhold, Klaus J Schnake, Frank Kandziora, Michael G Fehlings, Marcel F Dvorak, and Bizhan Aarabi. 2016. “AOSpine subaxial cervical spine injury classification system”. *European spine journal* 25 (7): 2173-84.

Viano, David C. and Chantal S. Parenteau. 2008. “Analysis of Head Impacts Causing Neck Compression Injury”. *Traffic Injury Prevention* 9 (2): 144-52. https://doi.org/10.1080/15389580801894940.

Wagnac, Eric, Carl-Éric Aubin, Kathia Chaumoître, Jean-Marc Mac-Thiong, Anne-Laure Ménard, Yvan Petit, Anaïs Garo, and Pierre-Jean Arnoux. 2017. “Substantial vertebral body osteophytes protect against severe vertebral fractures in compression”. *Plos one* 12 (10): e0186779.

Wagnac, Eric, Jean-Marc Mac-Thiong, Pierre-Jean Arnoux, Jean-Michel Desrosiers, Anne-Laure Ménard, and Yvan Petit. 2019. “Traumatic spinal cord injuries with fractures in a Québec level I trauma center”. *Canadian Journal of Neurological Sciences* 46 (6): 727-34.

White, Nicholas A., Paul C. Begeman, Warren N. Hardy, King H. Yang, Koshiro Ono, Fusako Sato, Koichi Kamiji, Tsuyoshi Yasuki, and Michael J. Bey. 2009. “Investigation of Upper Body and Cervical Spine Kinematics of Post Mortem Human Subjects (PMHS) during Low-Speed, Rear-End Impacts”. In . SAE International. https://doi.org/10.4271/2009-01-0387.

Yin, Sha, Jiani Li, and Jun Xu. 2017. “Exploring the mechanisms of vehicle front-end shape on pedestrian head injuries caused by ground impact”. *Accident Analysis & Prevention* 106: 285-96.

Yoganandan, Narayan A., Frank A. Pintar, Brian D. Stemper, M. B. Schlick, Mathieu M. G. M. Philippens, and Jac Wismans. 2000. “Biomechanics of Human Occupants in Simulated Rear Crashes: Documentation of Neck Injuries and Comparison of Injury Criteria”. *Stapp Car Crash Journal* 44: 189-204.

Yoganandan, Narayan, Cameron R Bass, Liming Voo, and Frank A Pintar. 2017. “Male and female cervical spine biomechanics and anatomy: implication for scaling injury criteria”. *Journal of biomechanical engineering* 139 (5).

Yukawa, Yasutsugu, Fumihiko Kato, Kota Suda, Masatsune Yamagata, and Takayoshi Ueta. 2012. “Age-related changes in osseous anatomy, alignment, and range of motion of the cervical spine. Part I: Radiographic data from over 1,200 asymptomatic subjects”. *European Spine Journal* 21 (8): 1492-98.